AD-A254 326

ON PAGE

Form Approved
OMB No. 0704-0188

...per response, including the time for reviewing instructions, searching existing data sources, ...ction of information. Send comments regarding this burden estimate or any other aspect of this ...shington Headquarters Services, Directorate for Information Operations and Reports, 1215 Jefferson ...avis Highway, Suite 1204, Arlington, VA 22202-4302, and to the Office of Management and Budget, Paperwork Reduction Project (0704-0188), Washington, DC 20503

1. AGENCY USE ONLY (Leave blank)	2. REPORT DATE	3. REPORT TYPE AND DATES COVERED
		FINAL 15 Nov 90 - 14 Nov 91

4. TITLE AND SUBTITLE
"INVESTIGATION OF HIGH EFFICIENCY MONOLITHIC MULTIBANDGAP SOLAR CELLS" (U)

5. FUNDING NUMBERS
61102F
2301/A7

6. AUTHOR(S)
Professor Larry Olsen

7. PERFORMING ORGANIZATION NAME(S) AND ADDRESS(ES)
Tri-Cities Univ Center
University of Washington
100 Sprout Road
Seattle, WA 98195

8. PERFORMING ORGANIZATION REPORT NUMBER
AFOSR-TR- 92 0[illegible]4

9. SPONSORING/MONITORING AGENCY NAME(S) AND ADDRESS(ES)
AFOSR/NM
Bldg 410
Bolling AFB DC 20332-6448

10. SPONSORING/MONITORING AGENCY REPORT NUMBER
AFOSR-91-0095

DTIC ELECTE AUG 17 1992 S D

11. SUPPLEMENTARY NOTES

12a. DISTRIBUTION/AVAILABILITY STATEMENT
Approved for public release;
Distribution unlimited

12b. DISTRIBUTION CODE
UL

13. This program involved investigations of AlGaAs/GaAs multijunction solar cells. Most of the low level effort was devoted to studies of the electronic properties of AlGaAs films. Finite diffusion lengths could only be obtained for Al(x)Ga(1-x)As films with the aluminum concentration in the range from 0 to 0.1. Photoresponse of Al/AlGaAs Schottky barriers were analyzed to measure minority carrier diffusion length (L). Values of L for p-type AlGaAs with x=0.1 were typically in the range of 0 to 0.5 um. It is clear that much more effort must be made to reduce oxygen and water impurity levels in the WSU barrel-type reactor before improved AlGaAs could be grown. An apparent bandgap shift implied by photoresponse data for Al/AlGaA Schottky barriers is explained as being due to improper mixing of Al and Ga precursors. Results are discussed for films grown with improved mixing which do not exhibit the apparent bandgap shift. Estimated performance for a two-cell, AlGaAs/GaAs structure are given based on characteristics of Al(.37)Ga(.63)As cells fabricated from wafers obtained from Varian, and GaAs cells fabricated for epi wafers grown with the WSU reactor.

14. SUBJECT TERMS	15. NUMBER OF PAGES
	25
	16. PRICE CODE

17. SECURITY CLASSIFICATION OF REPORT	18. SECURITY CLASSIFICATION OF THIS PAGE	19. SECURITY CLASSIFICATION OF ABSTRACT	20. LIMITATION OF ABSTRACT
UNCLASSIFIED	UNCLASSIFIED	UNCLASSIFIED	SAR

RNM 29 Jul 92
A

INVESTIGATION OF HIGH EFFICIENCY MONOLITHIC MULTIBANDGAP SOLAR CELLS

FINAL REPORT

For Period

11/15/90 - 11/15/91

AFOSR GRANT: AFOSR - 91 - 0095

START DATE: 11/16/90
CONTRACTOR: WASHINGTON STATE UNIVERSITY
(WSU Tri-Cities)

PRINCIPAL INVESTIGATOR: Dr. Larry C. Olsen

92-22709

92 8 1

ABSTRACT

This program involved investigations of AlGaAs/GaAs multijunction solar cells. Most of the low level effort was devoted to studies of the electronic properties of AlGaAs films. Finite diffusion lengths could only be obtained for $Al_xGa_{1-x}As$ films with the aluminum concentration in the range of $0 \leq x \leq 0.1$. Photoresponse of Al/AlGaAs Schottky barriers were analyzed to measure minority carrier diffusion length (L). Values of L for p-type AlGaAs with $x = 0.1$ were typically in the range of 0 to 0.5 μm. It is clear that much more effort must be made to reduce oxygen and water impurity levels in the WSU barrel-type reactor before improved AlGaAs could be grown. An apparent bandgap shift implied by photoresponse data for Al/AlGaAs Schottky barriers is explained as being due to improper mixing of Al and Ga precursors. Results are discussed for films grown with improved mixing which do not exhibit the apparent bandgap shift. Estimated performance for a two-cell, AlGaAs/GaAs structure are given based on characteristics of $Al_{.37}Ga_{.63}As$ cells fabricated from wafers obtained from Varian, and GaAs cells fabricated for epi wafers grown with the WSU reactor.

From 0 to 0.1

TABLE OF CONTENTS

DTIC QUALITY INSPECTED 5

Accession For
NTIS GRA&I
DTIC TAB
Unannounced
Justification
By
Distribution
Availability Codes
Dist
A-1

LIST OF FIGURES

1. INTRODUCTION

1.1 Research Objectives

This program has involved studies concerning a two-cell monolithic stack involving an AlGaAs and a GaAs solar cell as described in Figure 1. The overall objective was to investigate material science issues related to fabrication of a AlGaAs/GaAs two cell stack. Emphasis was placed on work concerning properties of AlGaAs films. Some effort was also directed towards fabrication and characterization of individual AlGaAs and GaAs solar cells that are appropriate for a two cell stack.

The theoretical efficiency of the AlGaAs/GaAs structure coupled to an AM1.5 solar spectrum is approximately 36.6 %. The individual cell theoretical efficiencies and characteristics are given in Table 1. Technology required for the GaAs cell has been developed. The key challenge rests with fabrication of the AlGaAs cell component. The reactive nature of the Al species makes it very difficult to grow AlGaAs films with adequate minority carrier diffusion lengths. O_2 or H_2O are usually residual impurities in process gases, and the strong nature of the Al-O bond ensures that oxygen present in the growth environment will be readily incorporated into a growing layer of AlGaAs. Once incorporated oxygen give rise to deep traps that are effective recombination centers, and thus cause reduced diffusion lengths. As a result, a primary objective of the program was to develop a better understanding of requirements for growth of AlGaAs with adequate minority carrier diffusion lengths.

TABLE 1

Theoretical Efficiency of Two-Terminal Two Cell Tandem Structure

Cell	Bandgap (eV)	Jsc (mA/cm2)	Voc (Volts)	Fill Factor	AM1.5G Efficiency (%)
$Al_{.37}Ga_{.63}As$	1.93	16.1	1.492	0.915	22.0
GaAs	1.42	16.1	1.016	0.890	14.6
			Total Efficiency		36.6

1.2 Technical Approach

The program involved activity in four areas:

- MOCVD growth of AlGaAs layers;
- Electronic properties of AlGaAs films;
- Fabrication and characterization of 1.93 eV AlGaAs cells;
- Fabrication and characterization of GaAs cells.

AlGaAs and GaAs films were grown with the WSU SPIRE 500XT MOCVD reactor housed at WSU Tri-Cities. Characterization of AlGaAs films involved determination of minority carrier diffusion length by analyzing the photoresponse of Schottky barriers, and by determining dopant concentration profiles with an electrochemical C-V profiler. Solar cells based on 1.93 eV AlGaAs were fabricated from epitaxial wafers grown by Varian Corp.. GaAs solar cells appropriate for the bottom cell in a two-cell stack were fabricated from epitaxial wafers grown with the WSU reactor.

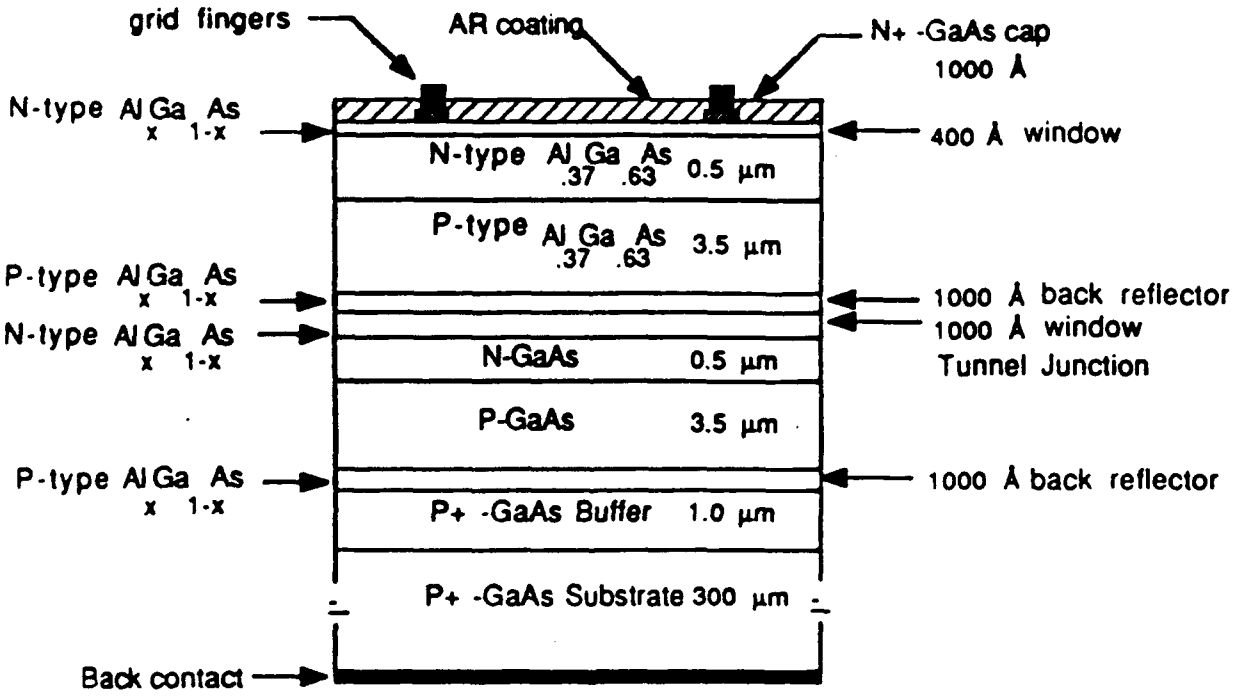

Figure 1. Structure of AlGaAs/GaAs Two - cell Monolithic Structure.

2. MOCVD GROWTH OF AlGaAs And GaAs EPITAXIAL LAYERS

2.1 WSU Tri-Cities MOCVD System

The growth system used for all of the films in this study utilizes an SPI-MOCVD™ 500XT vertical barrel reactor with a water-cooled double-walled quartz reaction chamber (in order to minimize any parasitic reactions). Each end of the reaction chamber is sealed by double concentric O-rings and a quadrupole mass spectrometer is used to detect any leaks in the seals. The growth pressure is controlled by a mechanical pump system, and the growth temperature is controlled via rf inductive heating of a graphite coated SiC susceptor. All reactor functions are computer controlled.

2.2 Growth of $Al_xGa_{1-x}As$ And GaAs Films

Trimethylgallium (TMGa) and trimethylaluminum (TMAl) were used as metalorganic sources for all AlGaAs film growths and pure AsH_3 served as the As source. GaAs films , of course, did not utilize TMAl. Silane was used as the n-type dopant gas and dimethylzinc as the p-type dopant source. Palladium-diffused H_2 flowing at a total of 9 liters/min was used as the carrier gas for all precursors. The $Al_xGa_{1-x}As$ films were grown on conductive <100> GaAs substrates misoriented 2° towards <110>. Once the substrate was loaded into the reactor it was heated to the growth temperature and kept under a flowing AsH_3/H_2 ambient for 15 minutes prior to growth to deoxidize the GaAs surface. The metalorganic sources were then introduced into the reactor and the epitaxial film was grown at a typical rate of 12 Å/sec to a thickness of approximately 4 μm. The V/III ratio was maintained at a value on the order of 50 for all growths and the reactor pressure was typically 80 torr.

2.3 Aluminum Composition by X-ray Analysis

X-Ray diffraction measurements have been utilized to determine AlGaAs film composition. Since the AlGaAs films were grown on <100> GaAs substrates an {004} reflection was examined using CuKα (λ=1.54Å) radiation. Knowing the lattice constants for GaAs and AlAs and making use of the Bragg Law and the plane spacing equation for a cubic [FCC] crystal, the Bragg angles of GaAs and AlAs can be determined for an {004} reflection. Using the Bragg angles of GaAs and AlAs as the scan range, the AlGaAs peak

would be measured because the lattice constant of AlGaAs is between the values for GaAs and AlAs (a linear relationship). Making use of the GaAs peak and the scan rate, the Bragg angle of the AlGaAs can be determined and thus the lattice constant. The lattice constant then leads to the composition. Figure 2 gives a plot of percentage AlAs versus TMAl flow as determined by XRD analysis. Shown for comparison is a line representing the theoretical compositions based on the partial pressures of the source precursors. There

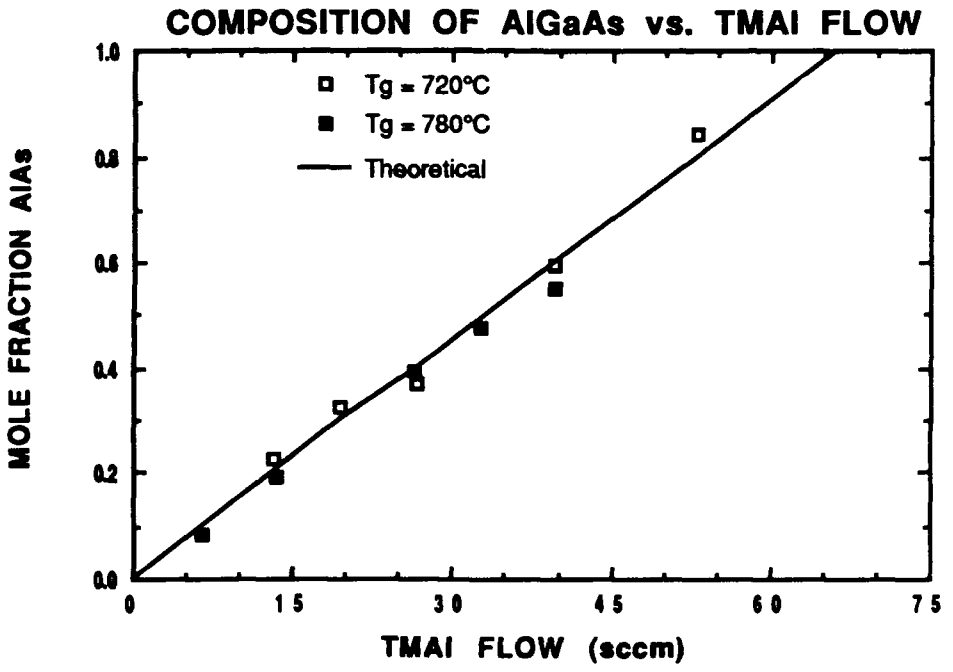

Figure 2. Mole fraction AlAs vs. flow of TMAl for W.S.U./Tri-Cities MOCVD reactor. The squares represent data obtained by x-ray analysis and the solid line represents theoretical calculations.

are several assumptions used in the theoretical calculations: a total reactor pressure of 80 torr; excess AsH_3; a Group III total pressure of 0.0222 torr; TMGa @ 0°C and 700 torr; TMAl @ 20°C and 700 torr; (Ga flow) =19.9- (0.3Al flow); TMAl existing as a dimer in the vapor phase. Note the generally good agreement between the experimental values and the theoretical calculations over the entire composition range.

3. ELECTRONIC PROPERTIES OF AlGaAs FILMS

3.1 Photoresponse Of Al/AlGaAs Schottky Barriers

Photoresponse of Al/AlGaAs Schottky barriers has been measured and analyzed to determine minority carrier diffusion length. The devices are fabricated such that the aluminum layer is thin enough to pass a significaqnt fraction of an incident flux of photons into the AlGaAs region. If photons of energy $h\nu \geq Eg$ are incident on a sample and each photon creates one electron-hole pair, the maximum possible photocurrent is given by

$$I_{max} = q \bullet F$$

where F is the incident photon flux. The two major contributions to the photocurrent of the Schottky barrier are due to current collected from the depletion region and from the bulk. The collection of current from the depletion region is essentially the same as in a p-n junction device. It is assumed that the high electric field present in the depletion region sweeps carriers out before they can recombine. As a result

$$I_{ph} = I(\text{Depletion Region}) + I(\text{Bulk})$$

where

$$I(\text{Depletion Region}) = qTF[1-\exp(-\alpha W)]$$

$$I(\text{Bulk}) = qTF\exp(-\alpha W)\,[\,\alpha L/(1+\alpha L)\,]$$

where T is the transmittance of photons through the metal film, F is the incident photon flux at a specific wavelength of light, α is the absorption coefficient, W is the depletion region width, and L is the minority carrier diffusion length. The reflection of light from the metal surface and adsorption in the metal film are accounted for in T.

The collection of current from the bulk of the Schottky barrier cell is essentially the same as from the base of a p-n junction device with a modification due to the transmittance being less than 100%. Collection of carriers from the bulk is dependent upon the minority carriers having sufficient lifetime (diffusion length) to diffuse to the depletion region. The above expression for I(Bulk) is based on the assumption that the back contact (contact other than the Schottky barrier) is ohmic and if the device thickness is much greater than the minority carrier diffusion length.

We define the external photoresponse of a Schottky barrier by the relationship

$$Iph = Q_{ext} \bullet I_{max}$$

From the above results, we have

$$Q_{ext} = T \bullet [1 - \exp(-\alpha W) + \exp(\alpha W) \bullet [\alpha L/(1+\alpha L)]]$$

The internal photoresponse (Q_{int}) is given by Q_{ext}/T. Q_{int} is independent of the film transmittance, and thus only depends on the AlGaAs properties. Figure 3a shows a photon flux F incident upon a Schottky barrier device with a short-circuit current being measured. Figure 3b depicts a band diagram of the same device showing electron hole pairs being created within the depletion region width, W, and also outside of the depletion region. Electron hole pairs created within the depletion region are immediately swept out by the high electric field present within the region, but in order for EHPs created outside this region to be collected the minority carriers (holes) must diffuse to

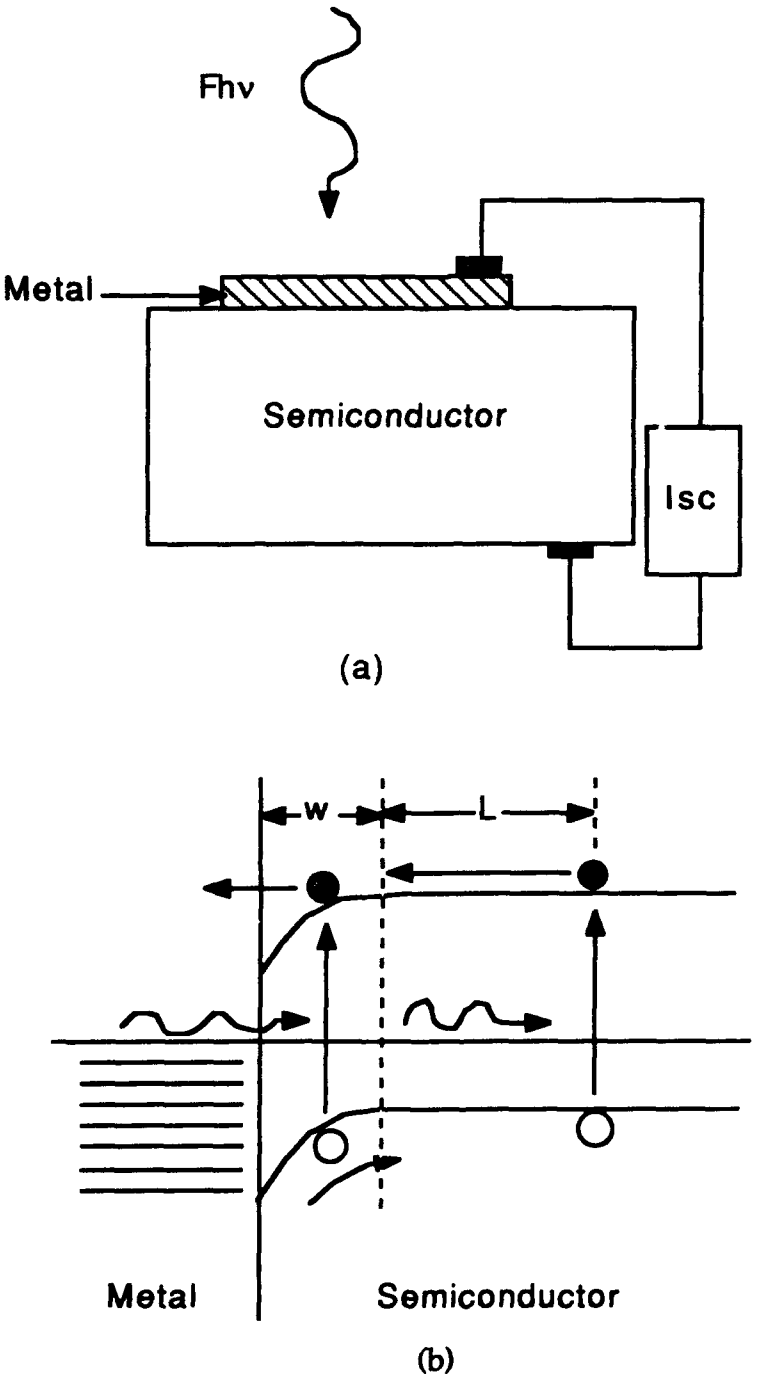

Figure 3. (a) Measurement of Short-Circuit Current for a Schottky Barrier Device; (b) The Associated Band Diagram

the depletion region. Thus, carriers must be created within the minority carrier diffusion length (L) in order to contribute to the photoresponse.

Schottky barriers were fabricated by depositing aluminum onto the semiconductor surface. In order to achieve acceptable sheet conductance and adequate transmittance, the thicknesses of aluminum films were limited to values between 70 and 95 Å. Thus, a typical deposition would last five or six seconds (the deposition rate being between 13 and 18 Å/sec). After deposition, the specimens were removed from the vacuum system, and ohmic contacts formed on the front surface of the device by mechanically applying (with teflon coated tweezers) small squares of indium and then alloying them with the semiconductor by applying heat locally. In some cases this simple method would not produce ohmic contacts requiring an additional "burn-in" step that involved passing a current of 0.15 mA (at 35 volts) between two squares of indium placed in close proximity on the semiconductor surface in addition to the previous steps.

In order to determine the optical properties (n and k values) of the Al film, transmittance (T) and reflectance (R) data were taken for quartz witnesses. The n and k of Al films were determined with a computer-aided analysis that utilizes values of T and R for each photon wavelength and the optical constants of quartz. After determining the optical properties of the Al film and measuring the photoresponse and reflectance of the Schottky barrier device, a data file was constructed that contained the n and k values of the Al film at each photon wavelength, the n and k values of the $Al_xGa_{1-x}As$ at each photon wavelength, the $Al_xGa_{1-x}As$ layer thickness, the depletion width, the thickness of a dead layer (see dead layer model), the diffusion length, the diffusivity of the $Al_xGa_{1-x}As$ (a constant), the back surface recombination velocity (assumed to be a constant for these devices), and the bandgap of the semiconductor. The data file was then entered into a modeling program that calculates the external (Q_{ext}) and internal (Q_{int}) photoresponse. The value of diffusion length is then varied until the calculated Q_{int} agrees with the measured Q_{int} at all wavelengths.

3.2 Dead Layer Model

We have found it necessary to include a "dead layer" at the front surface of the Schottky barrier devices in order to fit photoresponse data. In particular, to fit photoresponse data in the short wavelength region it was necessary to include a region located immediately beneath the Al metal that contributes no electron-hole pairs to the device current. The inclusion of this region assumes that electron-hole pairs generated within it flow in the wrong direction due to the Schottky effect (image force lowering), or that the region is intrinsic or n-type with a negligible minority carrier lifetime, as shown in Figure 4. Ga vacancies created by AsH_3 flow after cessation of growth and/or procedures leading up to and including the formation of the Schottky barrier may lead to type conversion at the AlGaAs surface. This is an area that needs further study to understand fully what is occurring.

Inclusion of the dead layer in modeling Schottky barrier photoresponse leads to the following:

$$I(\text{Depl Region}) = qTF \{ \exp(-\alpha d) - \exp(-\alpha W) \}$$

with d being the dead layer thickness.

3.3 Explanation Of Apparent Bandgap Shift

One effect that was present in photoresponse data taken on $Al_xGa_{1-x}As$ films grown during the last program and at the beginning of this effort, regardless of composition and diffusion length, was an apparent shift between the measured and theoretical bandgap appropriate for the intended composition of the $Al_xGa_{1-x}As$. The bandgap determined by photoresponse measurement was less than the theoretical bandgap of the intended material Figure 5 gives the internal photoresponse of a 10 % AlGaAs film which exhibited a bandgap shift typical of most ten-percent films. The magnitude of the bandgap shift was generally constant for a given intended composition, but not from composition to composition. Specifically, the shift observed in 10% films was usually 110 meV (theoretical E_g = 1.55 eV; measured E_g = 1.44 eV) and the discrepancy between theory and experiment increased with

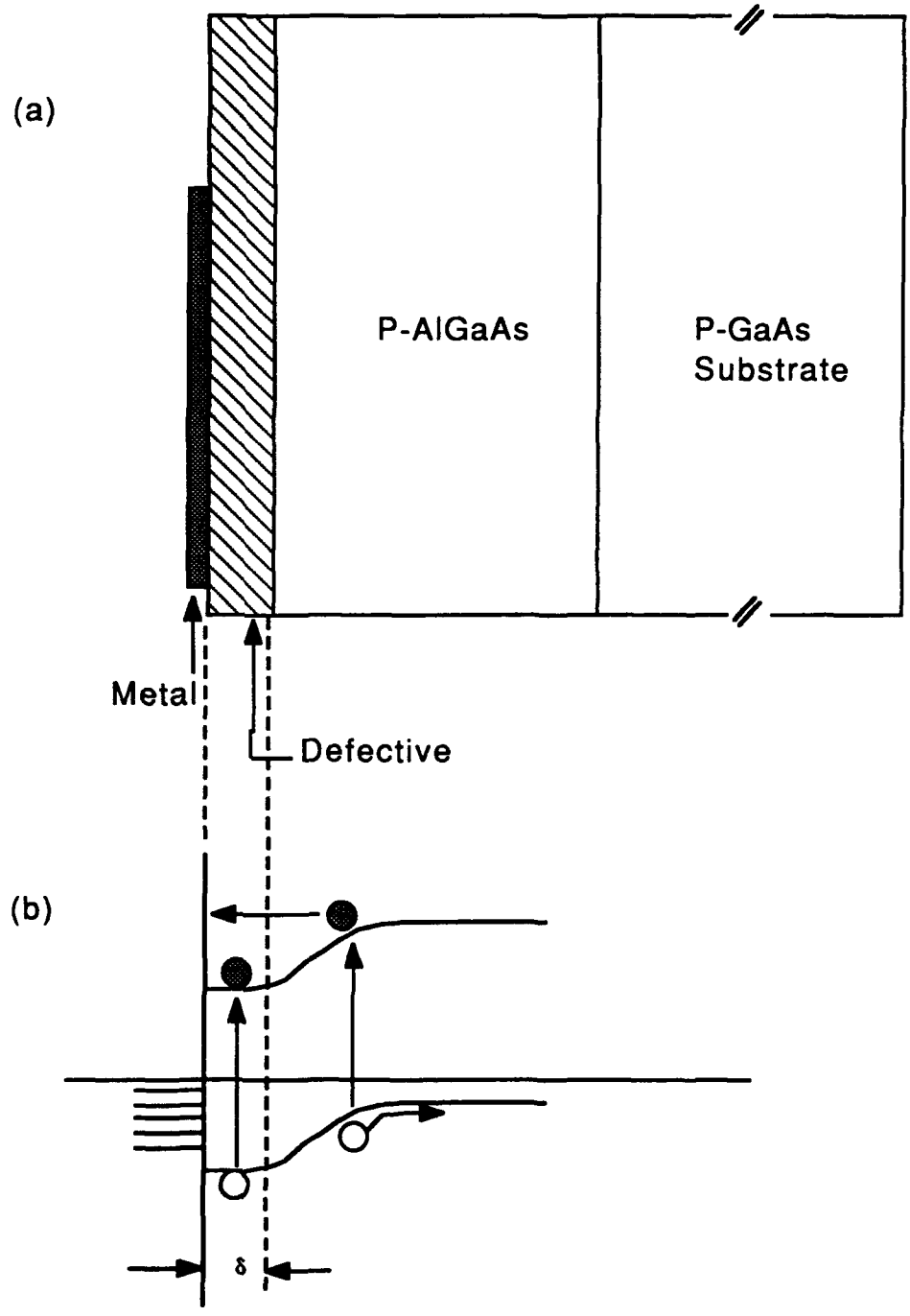

Figure 4. Dead Layer Model.

increasing Al content as shown in Figure 6. After investigating the problem in some detail, it appears that improper mixing of growth precursors in the WSU reactor has resulted in this problem.

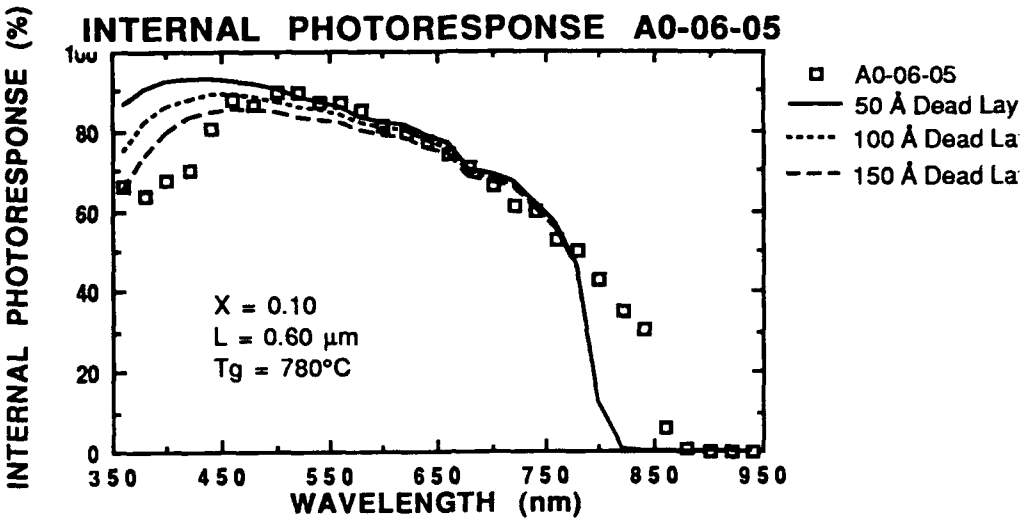

Figure 5. Internal Photoresponse vs. Wavelength For Specimen A0-06-05 (x = 0.1; p-type).

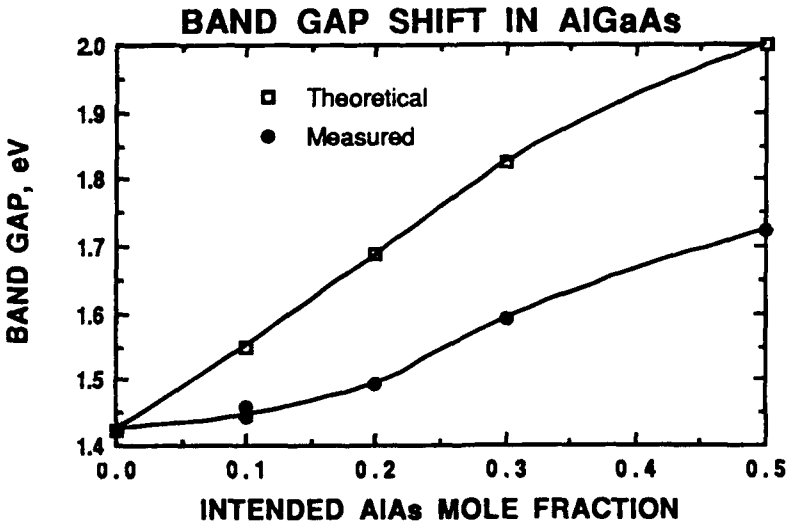

Figure 6. The theoretical and measured band gap versus intended AlAs mole fraction.

The primary reason for the observed behavior appears to be improper mixing of the growth precursors within the reaction chamber of the SPIRE 500XT MOCVD reactor causing alternating layers of high and low Al content material. A dopant concentration profile taken for an AlGaAs film is shown in Figure 7. The complete profile is given in Figure 7a, while an enlarged part of the profile is shown in Figure 7b. The sinusoidal fluxuations in composition can be related to the period of rotation of the susceptor. Since the substrate rests on a graphite susceptor within the reaction chamber that is rotating at four revolutions per minute and the typical growth rate for the $Al_xGa_{1-x}As$ films in this study is approximately 13 Å/sec, it can be calculated that approximately 195 Å of material is grown during each revolution. If the TMAl is not mixing well once it is injected into the reaction chamber by the radial injection manifold, then regions of low and high concentration of Al could exist near the susceptor. As the susceptor rotates the substrate through these regions, alternating layers of high and low Al content AlGaAs approximately 100 Å thick are grown, which in turn affects the efficiency which the p-type dopant Zn is incorporated into the film.

The mixing problem was solved by adding a baffle at the top of the reactor chamber that caused the gases to mix more effectively. Figure 8 shows modeled internal photoresponse data for a 10 % AlGaAs device for which the AlGHaAs film was grown with the baffle in place. Note the band edge is the same for both the experimental data and the calculated photoresponse. After the baffle was incorporated in the system, AlGaAs composition was more consistently homogeneous.

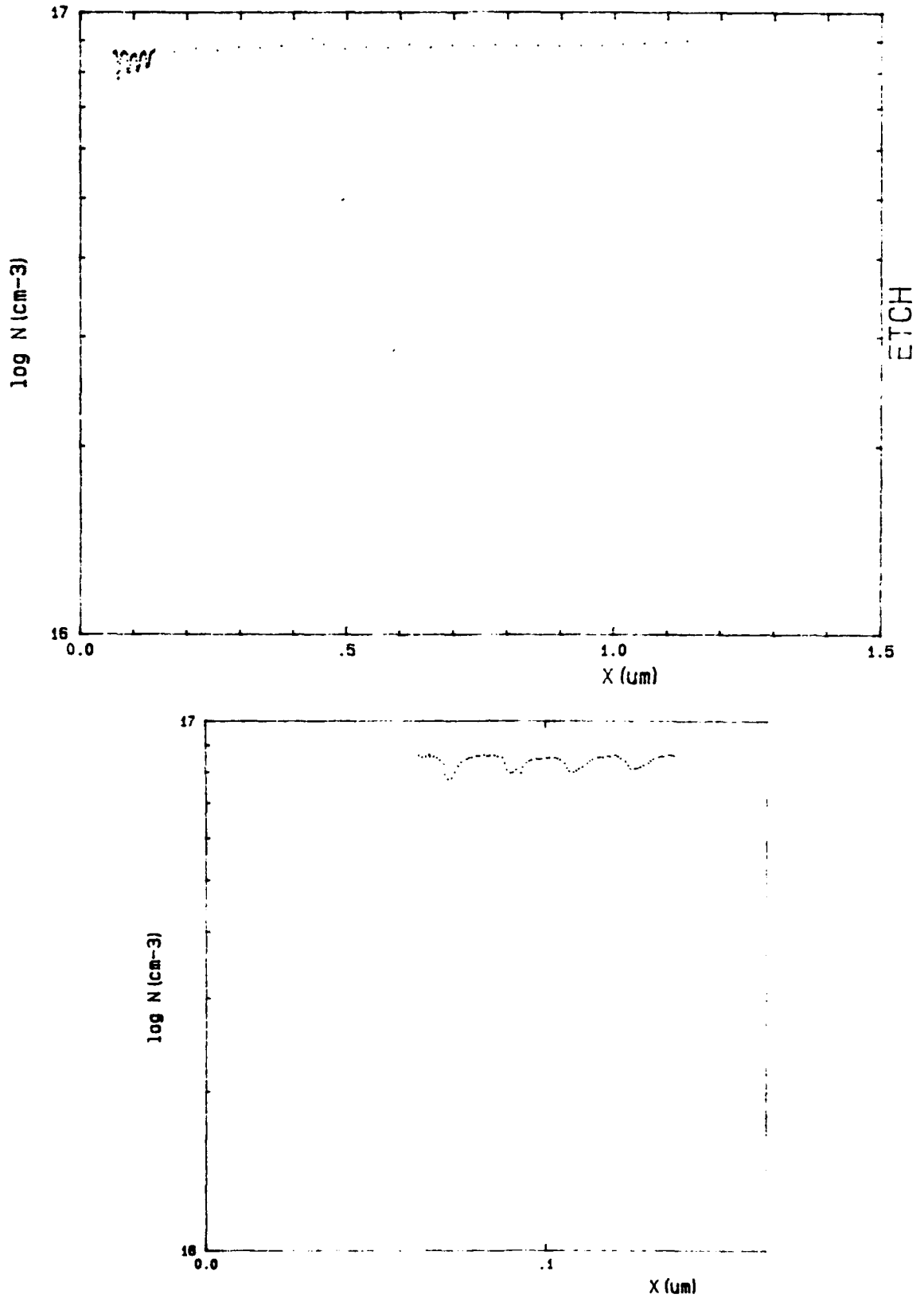

Figure 7. **(a)Polaron Profile For AlGaAs Film Grown On GaAs; (b). Enlarged View Of Profile Showing Oscillatory Behavior Of Carrier concentration.**

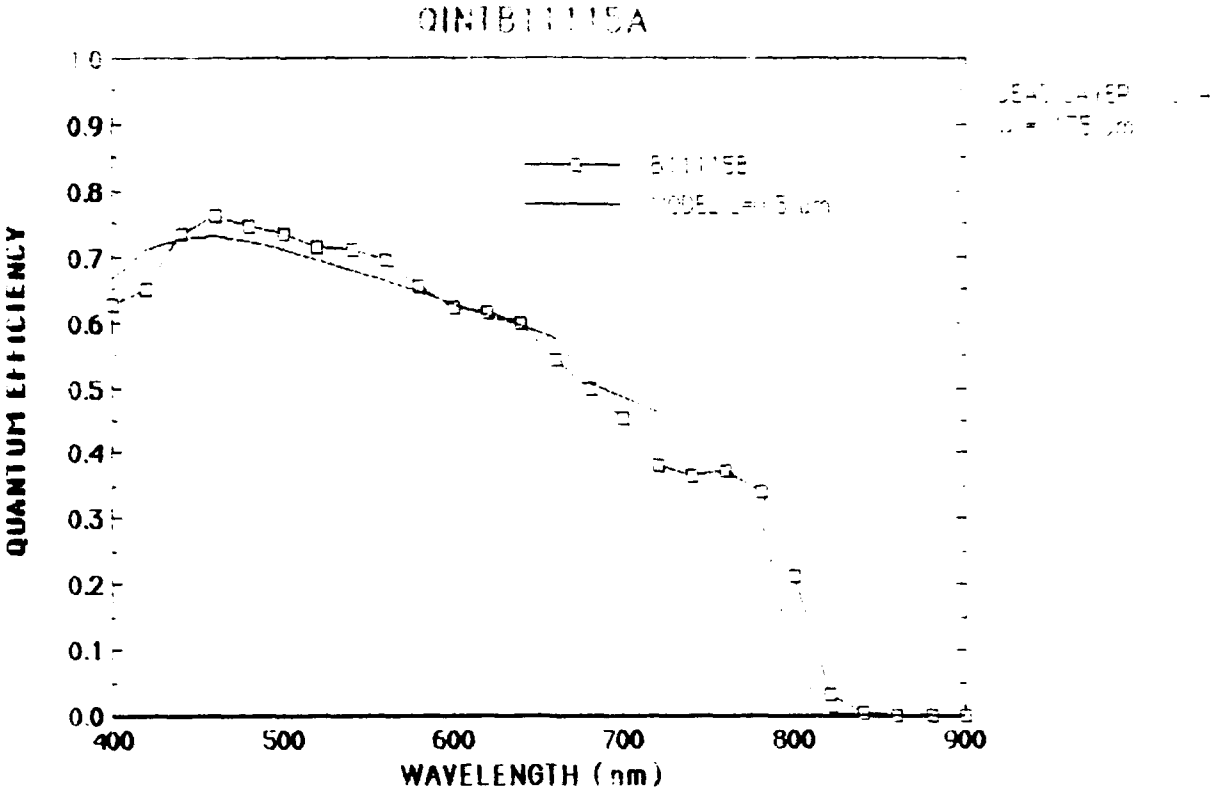

Figure 8. Modeled Internal Photoresponse For Al/p-AlGaAs Schottky Barrier For Which The AlGaAs Had 10 % Aluminum And Was Grown With Improved Mixing Of Precursors.

3.4 Minority Carrier Diffusion length Of AlGaAs Films

Minority carrier diffusion lengths of 10 % AlGaAs material never exceeded 0.6 to 0.8 μm during these investigations. Although this is a significant improvement over values of L obtained when the effort began, it is clear that additional measures are required in order to increase L to values obtained by the Varian group [1]. In particular, after discussing the problem with researchers at Varian, it would appear that we need to incorporate a purifier in every gas line entering the system to minimze the oxygen and water impurity levels. The cost of implementing this approach was prohibitive for this low level program.

4. FABRICATION AND CHARACTERIZATION OF 1.93 eV AlGaAs SOLAR CELLS

The electronic properties of AlGaAs grown with the WSU reactor have never reached the point that solar cell structures could be grown that exhibit reasonable efficiencies. The Electronic Materials group at WSU Tri-Cities was conducting another program during the same time period as this program that involved fabrication of AlGaAs solar cells from epi wafers grown by Varian Corporation. Thus, some of the effort of this program was directed towards fabrication and characterization of solar cells based on $Al_{.37}Ga_{.63}As$. Wafers with a layer structure depicted by Figure 9 were purchased (with funds from another program) from Varian and processed into solar cells. The graduate student supported by this program participated in cell fabrication and characterization. Wafers were diced into four die for 2.0 x 1.86 cm cells. Metallization on the front resulted in a collector grid with 40 lines/cm. Illuminated I-V characteristics obtained under simulated AM0 conditions are shown in Figure 10 This particular cell exhibited an AM0 efficiency of 13.7 %. The external photoresponse and reflectance versus wavelength are shown in Figure 11.

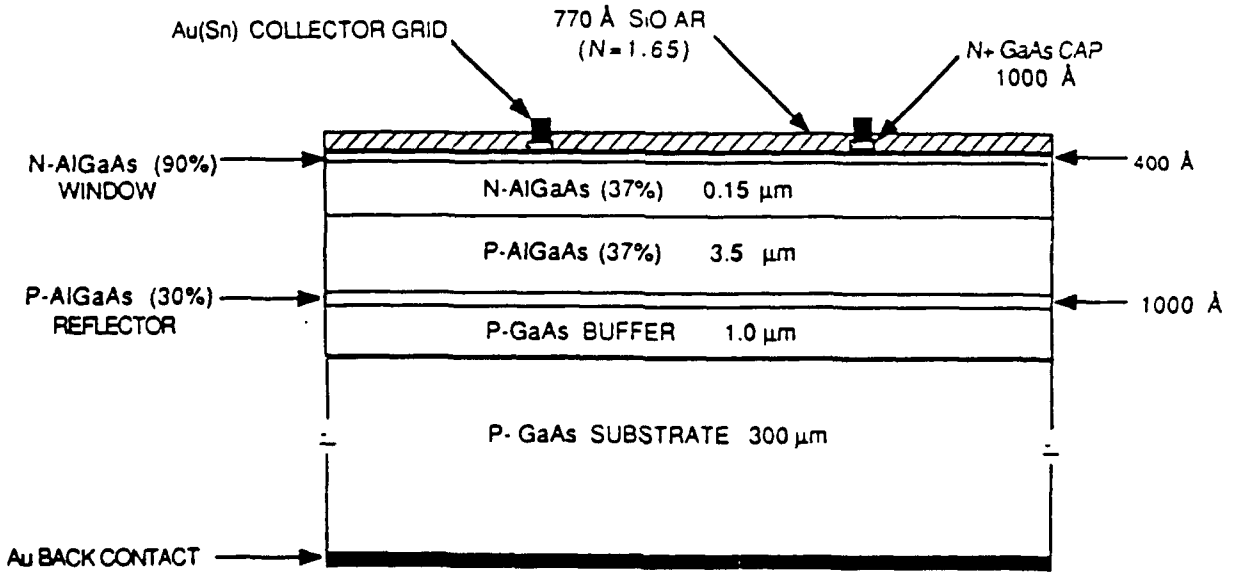

Figure 9. Layer Configuration Of An $Al_{.37}Ga_{.63}As$ Solar cell.

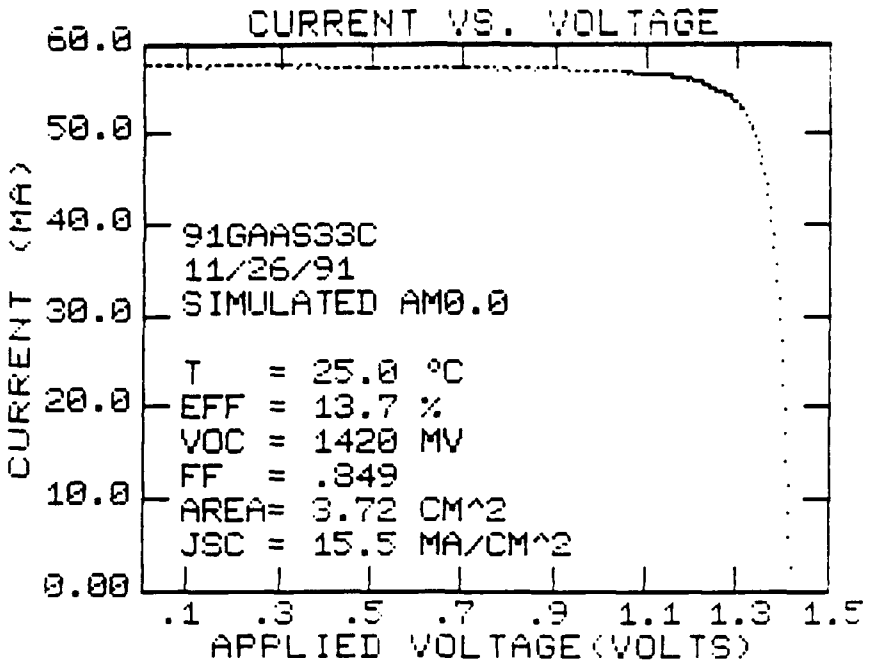

Figure 10. Simulated AM0 I-V Characteristics Of An $Al_{.37}Ga_{.63}As$ Solar cell Fabricated From A Varian Epi-Wafer.

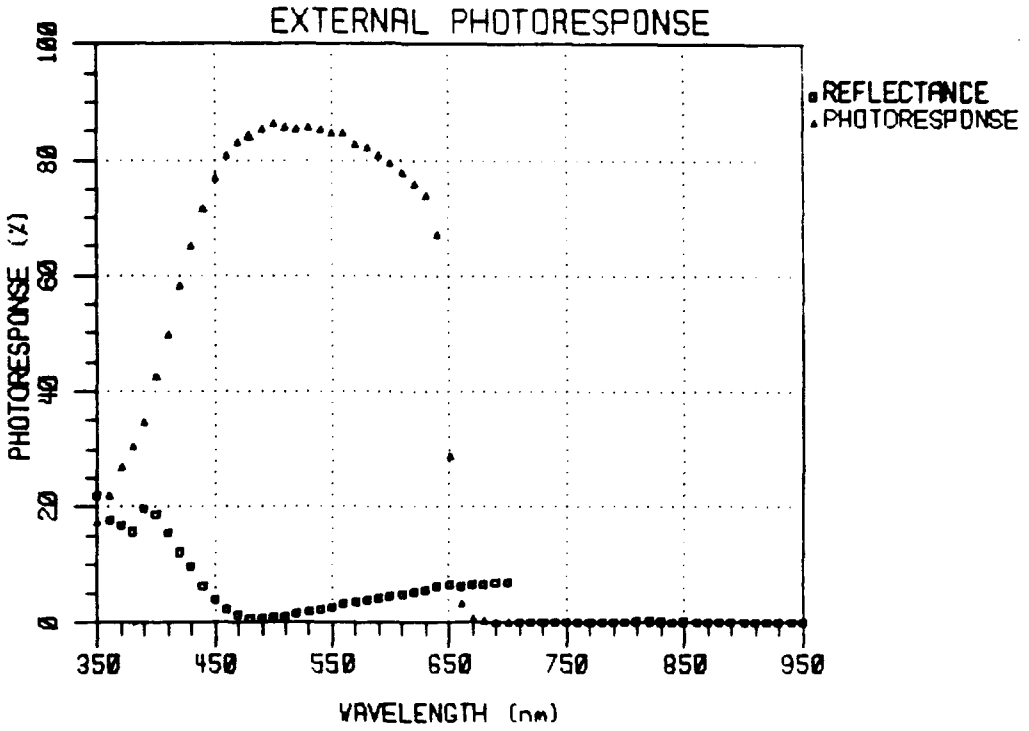

Figure 11. External Photoresponse For $Al_{.37}Ga_{.63}As$ Solar cell

5. FABRICATION AND CHARACTERIZATION OF GaAs CELLS FOR AN AlGaAs/GaAs TWO-CELL STRUCTURE

Some effort was also devoted towards fabrication and characterization of GaAs solar cells that have good response in the long wavelength region, as required by the bottom cell in a two-cell stack. This work was also done in conjunction with another low level program which was aimed at the development of GaAs solar cells for coupling to laser beams with wavelengths near 800 nm. The cell requirements are quite similar. For the AlGaAs/GaAs two-cell structure, it is desirable for the cell photoresponse to be as large as possible in the wavelength range of 650 nm to 850 nm. Clearly, the other application requires a large photoresponse at 800 nm.

Figure 12 depicts a p/n cell structure that is appropriate for both applications. The emitter is thicker than a broad band cell so that we can take advantage of the relatively large diffusion length of p-type material and maximize the photoresponse of the device in the long wavelength region. A depth concentration profile for a GaAs cell is shown in Figure 13. The figure plots the ionized donor or acceptor concentration versus distance. Figure 14 gives the external and internal photoresponse for a deep emitter cell. Note that the external photoresponse is $\geq$ 85 % for wavelengths $\geq$ 650 nm, which is important for a bottom cell in a two-cell stack. Figure 15 gives current-voltage characteristics of a cell illuminated under approximate AM1 conditions. The AM1 efficiency is 19.1 %. If the cell were used as a bottom cell and illuminated under AM1 conditions, the efficiency would be approximately 14 %. Combined with an AlGaAs cell that produces 14 %, the total two-cell efficiency would be 28 %.

Several cells with similar characteristics were fabricated from epi-wafers grown on the WSU MOCVD reactor (SPIRE 500XT). The front surface collector metallization was established using photolithography and liftoff of vapor deposited Au. Vapor deposited SiO (1000 Å) with an index of 1.75 was combined with the 500 Å AlGaAs window to provide a double AR coating yielding 0 % reflection at 806 nm.

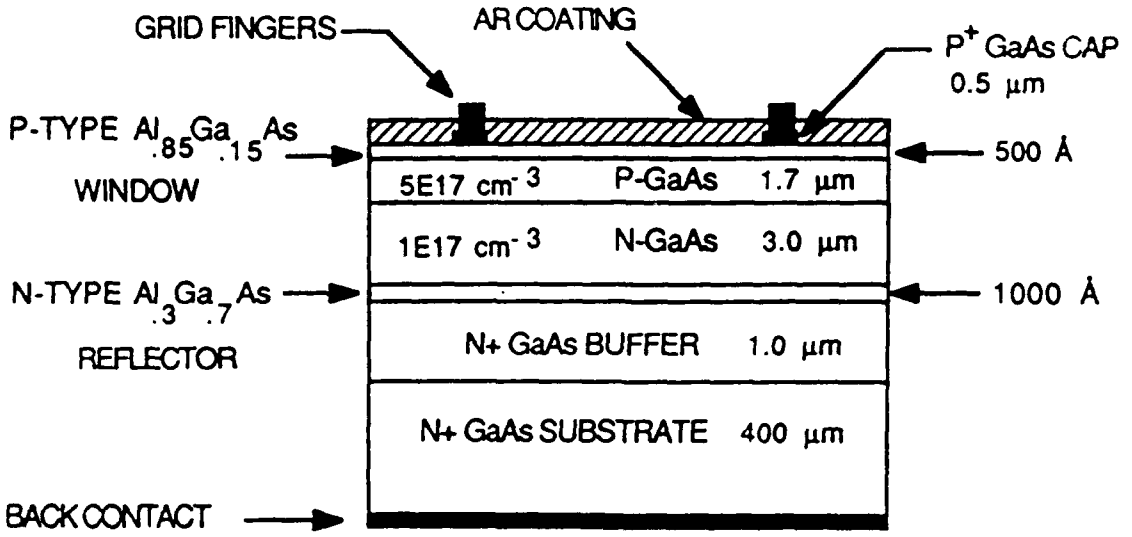

Figure 12. Layer Structure For GaAs Cell Design for Maximum Photoresponse In The Long Wavelength Range.

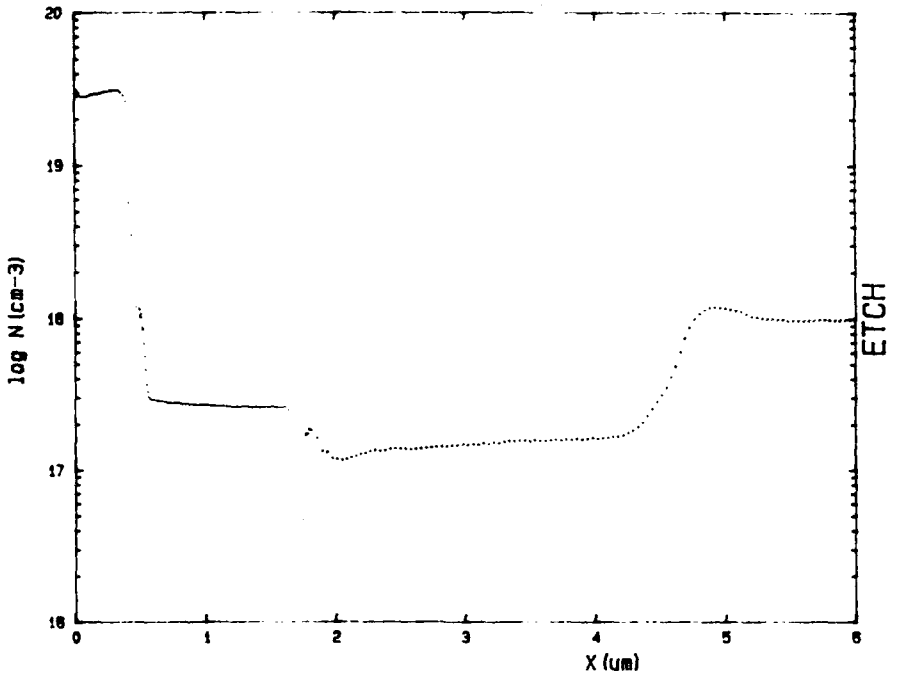

Figure 13. Polaron Profile For Deep Emitter Gaas Solar Cell.

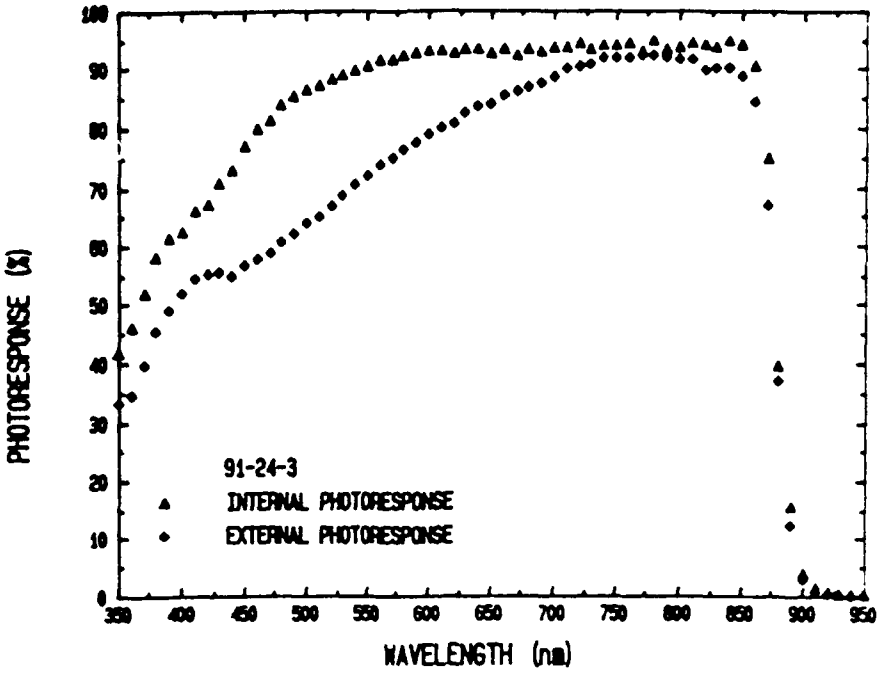

Figure 14. External And Internal Photoresponse For Deep Emitter GaAs Solar Cell.

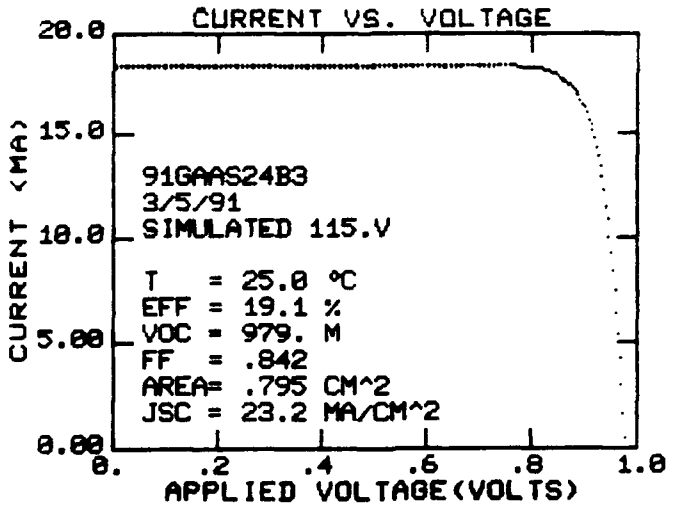

Figure 15. Current - Voltage Characteristics for GaAs Solar Cell Under Simulated AM1.5 Illumination.

6. CONCLUSIONS

The major objective of the program was to investigate material science issues concerning an AlGaAs/GaAs two-cell solar cell structure. The work was dominated by efforts to grow AlGaAs material that had adequate electronic properties for efficient solar cell fabrication. Most of the investigations centered on growth of $Al_{.1}Ga_{.9}As$ by MOCVD and determination of minority carrier diffusion length by analyzing the photoresponse of Al/p-AlGaAs Schottky barriers. Diffusion lengths in the range of 0.6 to 0.8 μm were obtained. Values ≥ 2.0 μm should be obtained. The WSU MOCVD system has only one gas line being filtered, namely, the hydrogen line. It would appear that in order to reduce oxygen and water contamination, all of the gas lines should be filtered.

In addition to the AlGaAs studies, some time was devoted to fabrication of AlGaAs and GaAs solar cells. Cells based on $Al_{.37}Ga_{.63}As$ were fabricated and characterized. The cells were fabricated from die derived from wafers grown by Varian.

GaAs solar cells appropriate for a bottom cell in an AlGaAs/GaAs two-cell system were fabricated. These devices were fabricated from epi-wafers grown with the WSU MOCVD reactor.

7. REFERENCES

1. M. J. Ludowise, and W.T. Dietze, J. Appl. Phys. 55, 4318 (1984).

APPENDIX

Publications:

"GaAs Solar cells For Laser Power Beaming," Conf. Proc., Space Photovoltaic Research And Technology, May 7 - 9, 1991, Page 26-1.

"High Efficiency Monochromatic GaAs Solar cells, " Proc. 22nd IEEE Photovoltaic Specialists Conf., page 419, Oct. 7 - 11, 1991.

"Effects Of Nonuniform Gas Mixing On Apparent Bandgap In 10 % AlGaAs Films", In Preparation.